Available online at www.sciencedirect.com
SCIENCE DIRECT®
Bioorganic & Medicinal Chemistry 12 (2004) 2035–2041
Bioorganic & Medicinal Chemistry

Homology modeling and molecular dynamics studies of a novel C3-like ADP-ribosyltransferase

Jing-fa Xiao, Ze-sheng Li* and Chia-chung Sun

Institute of Theoretical Chemistry, State Key Laboratory of Theoretical and Computational Chemistry, Jilin University, Changchun 130023, PR China

Received 11 September 2003; revised 27 February 2004; accepted 28 February 2004

Abstract—The novel C3-like ADP-ribosyltransferase is produced by a *Staphylococcus aureus* strain that especially ADP-ribosylates RhoE/Rnd3 subtype proteins, and its three-dimensional (3D) structure has not known. In order to understand the catalytic mechanism, the 3D structure of the protein is built by using homology modeling based on the known crystal structure of exoenzyme C3 from *Clostridium botulinum* (1G24). Then the model structure is further refined by energy minimization and molecular dynamics methods. The putative nicotinamide adenine dinucleotide (NAD^+)-binding pocket of exoenzyme $C3^{Stau}$ is determined by Binding-Site Search module. The NAD^+–enzyme complex is developed by molecular dynamics simulation and the key residues involved in the combination of enzyme binding to the ligand–NAD^+ are determined, which is helpful to guide the experimental realization and the new mutant designs as well. Our results indicated that the key binding-site residues of Arg48, Glu180, Ser138, Asn134, Arg85, and Gln179 play an important role in the catalysis of exoenzyme $C3^{Stau}$, which is in consistent with experimental observation.

1. Introduction

Various bacterial toxins are known to catalyze the transfer of the ADP-ribose moiety of nicotinamide adenine dinucleotide (NAD) onto specific target proteins of the eukaryotic cell. The mono-ADP-ribosylation is a post-translational modification of proteins catalyzed by enzyme that transfer the ADP-ribose moiety of NAD^+ to specific amino acids in protein acceptor.[1,2] The novel C3-like ADP-ribosyltransferase is produced by a *Staphylococcus aureus* strain (exoenzyme $C3^{Stau}$), which catalyzes the ADP-ribosylates of RhoE/Rnd3 subtype protein at the position of Asn-44 or catalyzes the ADP-ribosylates of Rho-A, -B, and -C proteins.[3] The Rho protein belongs to the Ras superfamily of low molecular mass GTPases, which are the major regulators of actin cytoskeleton, and they are also involved in the cell cycle progression and transcriptional activity.[4–6] A key issue in the search for novel molecules of pharmacological interest is their ability to hit an enzyme target selectively. Therefore, for rational drug design perspective, it is important to obtain detail knowledge of the site where the molecule is supposed to bind. More recently, the complexes of NAD-DT[7] and hydrolyzed NAD-ETA[8] have confirmed many conjectures regarding the NAD binding sites of DT and ETA, including the proximity of many catalytically important residues to the bound ligand. Structural comparison of proposed NAD biding site of several toxins shows that the spatial relationship of these key residues is more conserved in the different binding sites. Some experiments[9–11] explore the NAD binding site to C3 ADP-ribosyltransferases (including DT and PT) or C3 like ADP-ribosyltransferases, and indicate that the binding site may contain the key amino acid residues of Glu and Arg etc. Kahn and Bruice[12] investigate the mechanism of diphtheria toxin hydrolysis of NAD^+ by molecular dynamics study, and the results show that the charge relocalization is from the ribose ring through a hydrogen bond to Glu. Wilde et al.[13] report on the structure–function analysis of recombinant exoenzyme $C3^{Stau}$ that is based on site-directed mutagenesis. Their experimental results[13] display that Arg48, Arg85, Tyr175, Gln178, and Glu180 are essential for ADP-ribosyltransferase activity.

To our best knowledge, the 3D structure and the catalytic mechanism of exoenzyme $C3^{Stau}$ have not known. Therefore, in the present investigation, we construct a 3D model of the enzyme and search for the binding site of substrate. The 3D features of the model are obtained

Keywords: Homology modeling; Molecular dynamics; Docking; C3-Like ADP-ribosyltransferase.
* Corresponding author. Tel.: +86-4318-498984; fax: +86-4318-9459-42; e-mail: jingfaxiao@yahoo.com.cn

0968-0896/$ - see front matter © 2004 Elsevier Ltd. All rights reserved.
doi:10.1016/j.bmc.2004.02.038

by a homology modeling procedure based on the crystal structure of exoenzyme C3 (PDB code 1G24).[14] The homology model is an efficient method for the 3D structure construction of protein.[15] The model can be used to explain substrate specificity and relationship of enzyme function and structure. For this purpose, the docking simulation of the exoenzyme $C3^{Stau}$–NAD^+ complex is performed by Affinity module. The information on the NAD^+ binding domain of these enzymes is important for understanding the catalytic mechanism of ADP-ribosylation and can further help us to design the selective inhibitors.

2. Theory and methods

All calculations are performed on the SGI O3800 workstations using InsightII software package developed by Biosym Technologies.[16] In the energy minimization and molecular dynamical calculations, the consistent-valence forcefield (CVFF)[17] is employed. The secondary structures are assigned by using DSSP program.[18]

2.1. 3D model building

The Homology module[19] is used to build the initial exoenzyme $C3^{Stau}$ model. The homology protein is searched by Fasta program. A multiple sequence alignment is fulfilled based on the structural similarity among the templates with the aid of the Needleman–Wunsch algorithm.[20] The sequence identity between exoenzyme $C3^{Stau}$ and reference protein exoenzyme C3 from *Clostridium botulinum* (PDB code 1G24)[14] is 42%. An initial 3D structure of exoenzyme $C3^{Stau}$ is obtained by transferring the backbone coordinates of the exoenzyme C3 residues to the corresponding residues of exoenzyme $C3^{Stau}$, except for the several variable regions (LOOPs) as indicated in Figure 1. To construct the structural variable regions, a loop-searching algorithm over the databank of known crystal structure is used. The residues at the N-terminus end and C-terminus end are generated through end repair by using Insight/Homology program. Through the procedure mentioned above, an initial 3D model is thus completed.

The refinement of the homology model is obtained through energy minimization: 5000 iterations of steepest descent (SD) calculation are performed and then the conjugated gradient (CG) calculation is carried out until 0.1 kcal mol^{-1} $Å^{-1}$ of convergence on the gradient. After above simulations, the homology model is obtained by carrying out the molecular dynamics (MD) calculation with the use of Discover 3 software package.[21] MD simulations are carried out at 298 K. An explicit solvent model TIP3P water is used. The homology model is solvent with a 10 Å water cap from the center of mass of exoenzyme $C3^{Stau}$. Finally, a conjugate gradient energy minimization of full protein is performed until the root mean-square (rms) gradient energy is lower than 0.001 kcal mol^{-1} $Å^{-1}$. In this step, the quality of the initial

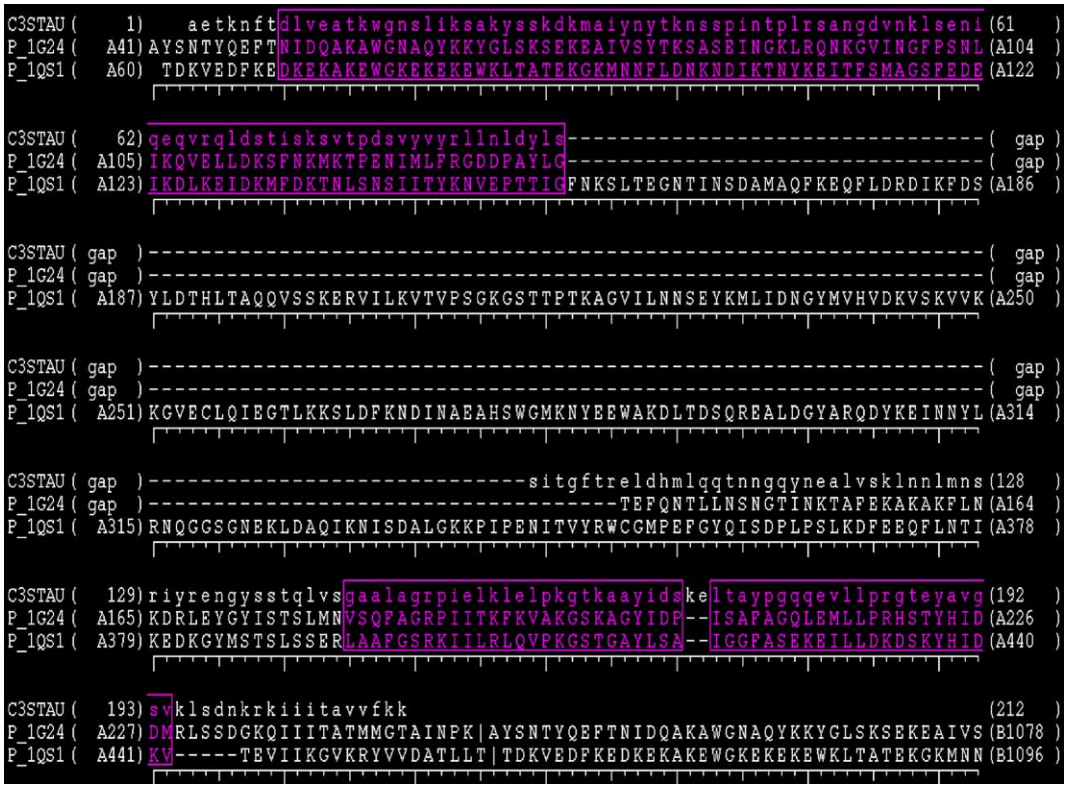

Figure 1. Multiple sequence alignment, with structurally conserved regions boxed, of exoenzyme $C3^{Stau}$ with two templates: exoenzyme C3 from *Clostridium botulinum* (PDB code: 1G24) and VIP2 (PDB code:1QS1).

model is improved. After the optimization procedure, the structure is checked by Profile-3D[22,23] and ProStat. The ProStat module of InsightII identifies and lists the number of instances where structural features differ significantly from the average values calculated from known proteins.

2.2. Binding site analysis

The Binding-Site module[24] is a suite of programs in InsightII for identifying and characterizing protein active sites, binding sites, and functional residues from protein. In this study, the Active Site-Search is used to search for the protein active site and binding site by locating cavities in the protein structure. First, the protein is mapped onto a grid, which covers the complete protein space. The grid points are then defined as free points and protein points. The protein points are grid points, within 2 Å from a hydrogen atom or 2.5 Å from a heavy atom. Then, a cubic eraser moves from the outside of the protein toward the center to remove the free points until the opening is too small for it to move forward. Those free points not reached by the eraser will be defined as site points. The binding site can be used to guide the protein–ligand docking experiment. The searched results are compared with the experiment given by Wilde et al.[13] to determine the NAD^+ binding site.

2.3. Docking the substrate into the active site

Molecular docking can fit molecules together with a favorable configuration to form a complex system. The structural information from the theoretical modeled complex can help us to understand the catalytic mechanism of enzyme. The 3D structure of NAD^+ is built with the Builder module. For tracking the interacting mode of exoenzyme $C3^{Stau}$ with NAD^+, the advanced docking program Affinity[25] is used to fulfill the automated molecular docking. The best binding structure of the ligand to the receptor based on the energy of the ligand/receptor complex is automatically found by Affinity, which uses a combination of Monte Carlo type and stimulated annealing procedure to dock a gust molecule to a host one. A key feature is that the 'bulk' of the receptor, defined as the atoms, which is not in the binding site specified, holds rigid during the docking process, while the atoms in binding site and ligand are moveable. The potential function of the complex is assigned by using the CVFF and the cell multipole approach is used for nonbond interactions. To account the solvent effect, the centered enzyme–ligand complexes are solvated in a sphere of TIP3P water molecules with radius 10 Å. The residues of Glu180 and Glu101 are modeled as anion. Finally, the docked complexes of exoenzyme $C3^{Stau}$–NAD^+ are selected according to the criteria of interacting energy combined with geometrical matching quality. These complexes are used as the starting conformation for further energetic minimization and geometrical optimization before the final models are achieved.

3. Results and discussion

3.1. Homology modeling of exoenzyme $C3^{Stau}$

Two reference proteins, exoenzyme C3 from *C. botulinum* (C3bot),[14] and vegetative insecticidal protein2 (VIP2),[26] are used to model the structure of the novel C3-like ADP-ribosyltransferase. The homology scores for the two reference proteins compared with exoenzyme $C3^{Stau}$ are 42% and 32%, respectively. The exoenzyme C3bot and VIP2 have the ADP-ribosyltransferases activity, which catalyzes the ADP-ribosylates of Rho-A, -B, and -C proteins. A similar mechanism is most likely functioning in the exoenzyme $C3^{Stau}$, exoenzyme C3bot, and VIP2. The homology of function can ensure the accuracy of the sequence alignment. In order to define structural conservative regions (SCRs) of the protein family, the multidimensional alignment is used to superimpose the two reference structures, and the five SCRs are determined (see Fig. 1). The Needleman–Wunsch algorithm with the identity matrix is used to align the amino acid sequence of exoenzyme $C3^{Stau}$ to the SCRs. By comparison, we choose the most similar reference protein exoenzyme C3bot[14] as the template protein for modeling exoenzyme $C3^{Stau}$. The LOOPs between SCRs are more variable in conformation among the reference protein. The loop-searching algorithm is used to construct the structure of LOOPs. The side chain conformations are selected to add to a protein backbone based on a backbone-dependent rotamer library and the optimum conformation is defined as that with the lowest nonbond energy. The structural optimization is proceeded by using energy minimization and molecular dynamics methods and the final structure of exoenzyme $C3^{Stau}$ is presented in Figure 2. From Figure 2 we can see that the enzyme has 7 helices and 10 sheets. The structure has been further checked by profile 3D and ProStat. For the exoenzyme $C3^{Stau}$ model, the stereochemical quality is checked by ProStat and there is not the case appeared that the bond lengths and bond

Figure 2. The Final 3D-structure of exoenzyme $C3^{Stau}$. The structure is obtained by energy minimizing an average conformation over the last 100 ps of MD simulation. The α-helix is represented by red color and the β-sheet is represented by yellow color.

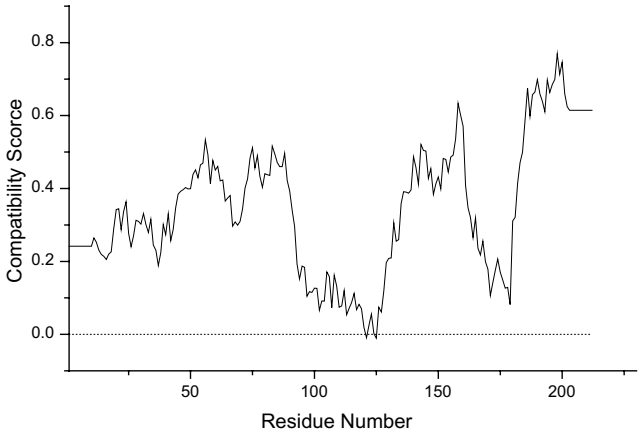

Figure 3. The 3D profiles verified results of exoenzyme C3^{Stau}, residues with positive compatibility score are reasonably folded.

angles are different significantly from the average values calculated from known proteins in the total residues. The compatibility between the amino acid sequence and the environment of the amino acid side chains in the model is another validation criterion. Here its compatibility scores are obtained by using Profile 3D and corresponding results for the exoenzyme C3^{Stau} model are shown in Figure 3. Note that compatibility scores above zero correspond to 'acceptable' side chain environment. From Figure 3, we can see that all residues are reasonable, which make us to believe that the structure of exoenzyme C3^{Stau} is reliable. Figure 4 shows the structure alignment of Ca trace between exoenzyme C3^{Stau} (model in vacuum), exoenzyme C3^{Stau} (model in account solvent effect), and template protein exoenzyme C3bot. The root mean square deviation of the Ca atoms (Ca RMSD) between exoenzyme C3^{Stau} (model in vacuum) and exoenzyme C3^{Stau} (model in account solvent effect) is 3.13 Å, which indicates that the solvent effect has some influences on the model structure. So the solvent effect must be take into account in the molecular simulation. It has been shown that the deviation of the Ca atoms between the template protein and the model protein is a good method of validation.[27] In the work, the Ca RMSD for all residues from the best model of exoenzyme C3^{Stau} to the corresponding atoms in the crystal structure of template protein exoenzyme C3bot is 3.89 Å.

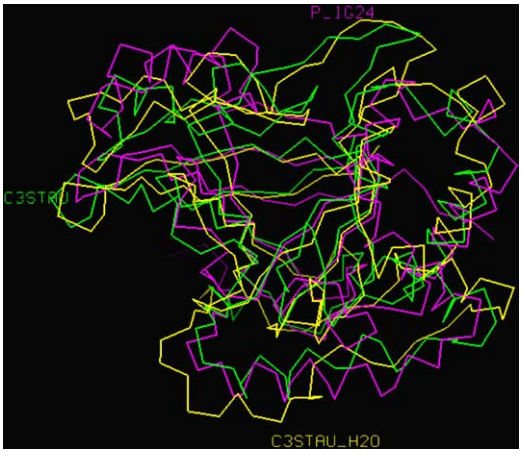

Figure 4. Ca trace of exoenzyme C3^{Stau} (model in vacuum represented by green color), exoenzyme C3^{Stau} (model in account solvent effect represented by yellow color), and template protein exoenzyme C3bot (in purple color) produced using structure alignment.

3.2. Determination of the NAD$^+$ binding pockets

The exoenzyme C3^{Stau}, exoenzyme C3 from *C. botulinum*, and VIP2 are well conserved in both sequence and structure, and their biological functions are also identical. In order to simulate the interaction between the exoenzyme C3^{Stau} and the substrate, the binding site is searched by Binding-Site module, which can be used to guide the protein–ligand docking experiment. By this process, two possible active sites are searched by the Binding-Site module and they are listed in Figure 5a and b. Site1 (in Fig. 5a) includes Ser41, Asn44, Thr45, Arg48, Ser49, Arg85, Leu87, Tyr91, Thr96, Thr99-Lys-Glu101, Ser138-Thr-Gln140, Arg150, Tyr175, Glu180, and Tyr189. Site2 (in Fig. 5b) includes

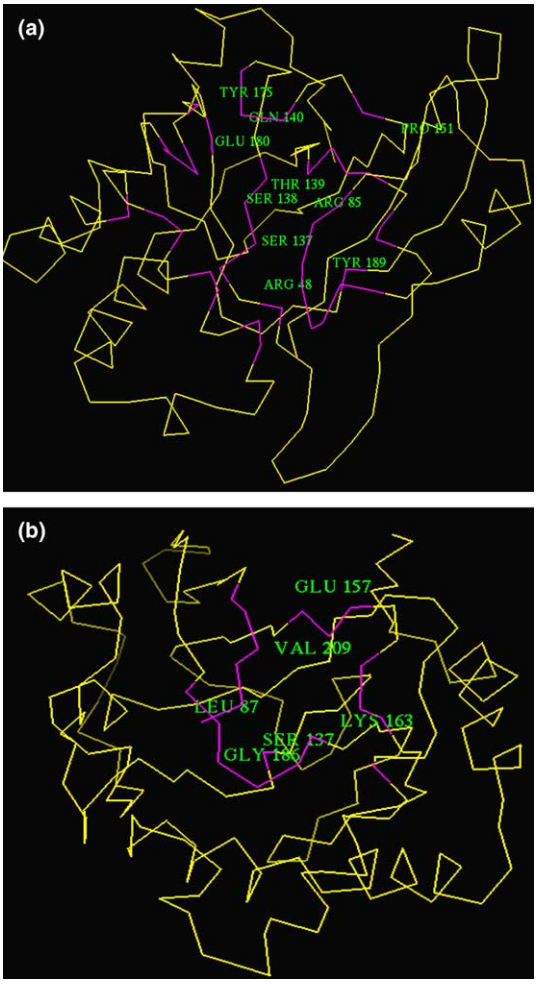

Figure 5. (a) The possible site1 is searched by the Binding-Site module. (b) The possible site2 is searched by the Binding-Site module. The key residues are labeled by green color.

Ser137, Glu157-Leu-Pro159, Thr162-Lys-Ala164, Leu183-Phe-Arg-Gly-Thr-Glu188, A207-Val-Val-Phe-Lys211, and Lys212. From the locations of the two sites, we can see that the sites are all in general depressions in the protein surface. After analyzing the properties of the residues in two sites and their locations, respectively, we think that the site1 is hydrophilic surfaces and as the receptor–ligand binding sites, the site1 is characteristically more deep. The result of sequence alignment (in Fig. 1) of exoenzyme $C3^{Stau}$ compared with exoenzyme C3 from *C. botulinum* reveals several conserved residues: a conserved glutamate (Glu180), termed as the 'catalytic glutamic acid'; the 'STS' motif, known to be critical for the enzyme activity of several ADP-ribosylating toxins, which is changed to an 'STQ' motif (Ser138-Thr139-Gln140) in exoenzyme $C3^{Stau}$.[28] Moreover, Arg48 and Arg85 in exoenzyme $C3^{Stau}$ are conserved between C3-like ADP-ribosyltransferases. For the final decision on the binding site, the searched result are compared to the experimental study by Wilde et al.[13] Indeed, the structure–function analysis of exoenzyme $C3^{Stau}$ based on site-directed mutagenesis by Wilde et al. indicates that the residues of Arg48, Arg85, Tyr175, Gln178, and Glu180 play an essential role for ADP-ribosyltransferase activity of exoenzyme $C3^{Stau}$. The experimental result[13] demonstrates that the site1 is the more reasonable binding site to dock NAD^+ and will be used in the further discussion. The site1 of substrate is a long and deep cleft between N-terminal α-helical moiety and the C-terminal β-sheet moiety of exoenzyme $C3^{Stau}$. This kind of binding site is similar to the homologous enzyme Ecto-ADP-ribosyltransferase 2.2 from rat (rAR2.2).[29]

3.3. Interaction between exoenzyme $C3^{Stau}$ and NAD^+

The 3D structure of NAD^+ is built with the Builder model. The molecular structure of NAD^+ consists of an adenosine biphosphate, ribose ring, and nicotinamide. In order to understand the interaction between exoenzyme $C3^{Stau}$ and NAD^+, the complex of exoenzyme $C3^{Stau}$–NAD^+ is developed by Affinity module. The probable binding 3D conformation of the exoenzyme $C3^{Stau}$–NAD^+ complex is shown by Figure 6. This figure shows that the NAD^+ locates in the center of the binding pocket, which is stable by the hydrogen bond and electrostatic interactions.

One important character of the interaction between exoenzyme $C3^{Stau}$ and NAD^+ is the hydrogen bonding interaction (Fig. 7 and Table 1). Hydrogen bonds play an important role for structure and function of biological molecules, especially for the enzyme catalysis. From Figure 7 and Table 1, we know that there are several hydrogen bonds are formed between the NAD^+ and some residues of exoenzyme $C3^{Stau}$. The two hydrogen bonds are formed between the main-chain carboxyl O of Asn134 and side-chain NH of Arg48 with adenosine group of NAD^+. And the side-chain OH of Ser138 forms one hydrogen bond with phosphate group of NAD. The nicotinamide group of NAD^+ is tightly bound via three hydrogen bonds with the side-chains carboxyl of Glu180, main-chain carboxyl O and main-chain NH of Gln179. The nicotinamide ribose is fixed by Glu180, which forms a tight hydrogen bond to the 2′-hydroxyl group. This network of hydrogen bonds in the catalytic site of exoenzyme $C3^{Stau}$ must play a vital role in determining the level of binding affinities in exoenzyme $C3^{Stau}$–NAD^+ complex. These hydrogen bonding interactions may enhance the stability of NAD^+–enzyme complex. On the further inspection of the exoenzyme $C3^{Stau}$–NAD^+ complex model, the

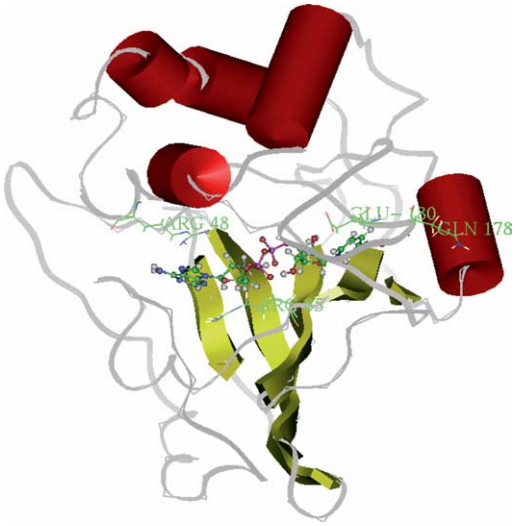

Figure 6. A stereo picture of the 3D-structure of complex NAD^+–exoenzyme $C3^{Stau}$.

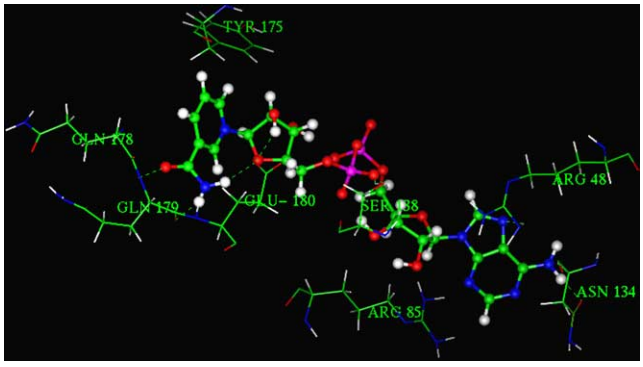

Figure 7. The hydrogen bonding interaction of complex NAD^+–exoenzyme $C3^{Stau}$.

Table 1. The hydrogen bonds between NAD^+ and binding pocket residues of exoenzyme $C3^{Stau}$

Exoenzyme $C3^{Stau}$		NAD^+ atom	Distance (Å)	Angle (deg)
Residue	Atom			
Glu180	O	Ribose OH	2.45	145.3
Arg48	NH	Adenosine N	2.10	138.6
Ser138	OH	Phosphate O	1.73	157.1
Asn134	O	Adenosine NH	1.99	149.6
Gln179	O	Nicotinamide NH	1.84	155.6
Gln179	NH	Nicotinamide O	2.09	132.9
Glu180	O	Nicotinamide NH	1.85	160.2

Glu180 is located adjacent to the ribose and is the only residue conserved in all known ADP-ribosyltransferase, which is equivalent to Glu189 of rAR2.2,[29] Glu148 of diphtheria toxin,[30] Glu553 of *Pseudomonas exotoxin* A,[31] and Glu129 of pertussis toxin.[32,33]

To determine the key residues that comprise the binding pocket of the model, the interaction energy of the substrate with each individual amino acid in the enzyme is also calculated. Significant binding-site residues in the models are identified by the total interaction energy between the substrate and each amino acid residues in the enzyme. The interaction energies correspond only to the enthalpic contributions to the free energy of binding. Moreover, since this model structure corresponds to homology modeling structure, the absolute values of these energies could also vary. However, even with these qualifications, the relative importance of each residue can be inferred by its rank order of interaction energy.[34,35] This identification, compared with a definition based on the distance from the substrate, can clearly show the relative significance for every residue. Table 2 gives the interaction energies including the total, van der Waals, and electrostatic energies with the total energy lower than -1.00 kcal mol^{-1} for all residues in exoenzyme C3^{Stau} with NAD$^+$. This table shows that there is large favorable total interaction energy for the enzyme–NAD$^+$complex and the total interaction energy is -162.79 kcal mol^{-1}. The van der Waals and electrostatic energies are -65.90 and -96.89 kcal mol^{-1}, respectively. It means that the interaction is mainly attractive interaction. Thus we can conclude that in this case both the van der Waals and electrostatic energies are important for determining the binding orientations. From Table 2 we also know that Ser138, Arg85, Tyr175, Arg150, Arg48, Gln140, Asn134, Asn44, Gln179, Ser137, Glu180, and Leu172 are important to anchor residues for the substrate NAD$^+$ and have main contributions to the substrate interactions. The total interaction energy, E_{total}, between the NAD$^+$ and Ser138 is -15.68 kcal mol^{-1} in which the primary interaction energy is electronic interaction one ($E_{ele} = -11.51$ kcal mol^{-1}). The residues of Arg150, Arg48, Asn44, Gln179, and Glu180 have the similar behavior as Ser138 and the interaction energies of these residues with NAD$^+$ are mainly contributed by electronic interaction. But, for the residue of Leu172, the interaction energy with NAD$^+$ is mainly contributed by van der Waals interaction. Arg48 and Arg85 of exoenzyme C3^{Stau} are equivalent with Arg51 and Arg88 of exoenzyme C3bot,[14] respectively. In the structure of both enzymes, these arginine residues are part of a polar pocket in which adenine ring of NAD$^+$ fits. The residue of Arg48 forms a hydrogen bond with adenine ring and the guanidinium group of Arg85 makes π–π interactions with adenine ring.[29] These residues of Arg48, Glu180, Ser138, Asn134, and Gln179 have large interaction energy with NAD$^+$ and they form hydrogen bonds with NAD$^+$ simultaneity. Thus we can conjecture that these residues are important residues for the binding of substrate-NAD$^+$ with exoenzyme C3^{Stau}, which is confirmed by Wilde et al.'s experimental investigation.[13] The energy information in Table 2 may guide the selection of candidate sites for further experimental studies on site-directed mutagenesis.

Table 2. The total energy (E_{total}), van der Waals energy (E_{vdw}), and electrostatic energy (E_{ele}) between NAD$^+$ and individual residues ($|E_{total}| > 1$ kcal mol^{-1} listed in energy rank order)

Residue	E_{vdw} (kcal mol^{-1})	E_{ele} (kcal mol^{-1})	E_{total} (kcal mol^{-1})
Total	−65.90	−96.89	−162.79
Ser138	−4.17	−11.51	−15.68
Arg85	−7.15	−7.41	−14.56
Tyr175	−3.04	−6.52	−9.56
Arg150	−0.48	−8.61	−9.09
Arg48	0.23	−9.03	−8.81
Gln140	−3.17	−5.53	−8.70
Asn134	−2.70	−5.23	−7.93
Asn44	−0.93	−5.90	−6.83
Gln179	0.54	−6.58	−6.04
Ser137	−2.30	−3.61	−5.91
Glu180	0.70	−6.28	−5.58
Leu172	−3.83	−1.55	−5.38
Ser40	−0.43	−4.66	−5.09
Leu147	−2.83	−1.86	−4.69
Leu87	−2.89	−1.49	−4.38
Thr139	−2.66	−1.39	−4.05
Gln178	−1.82	−1.96	−3.78
Gly177	−0.35	−3.16	−3.51
Gly135	−0.77	−2.41	−3.18
Tyr189	−2.67	−0.11	−2.78
Thr99	−0.59	−2.07	−2.66
Asn88	−0.23	−2.42	−2.65
Thr96	−2.73	0.36	−2.37
Arg100	−0.19	−2.16	−2.35
Ile43	−0.07	−1.97	−2.04
Leu47	−0.10	−1.92	−2.02
Thr173	−0.37	−1.62	−1.99
Leu86	−1.54	−0.43	−1.97
Tyr91	−0.92	−0.82	−1.74
Pro176	−2.15	0.67	−1.48
Glu153	−0.04	−1.29	−1.33
Tyr36	−0.61	−0.63	−1.24
Leu183	−0.12	−1.01	−1.13
Lys121	−0.31	−0.76	−1.07
Gly97	−0.75	−0.27	−1.02
Glu133	−0.30	−0.71	−1.01

4. Conclusions

The three-dimensional structure of the novel C3-like ADP-ribosyltransferase produced by a *S. aureus* strain (exoenzyme C3^{Stau}) has not known. In this investigation, the protein 3D structure is built by using homology modeling based on the known crystal structure of exoenzyme C3 from *C. botulinum* (1G24). Then the model structure is refined by the energy minimization and molecular dynamics methods. The putative NAD$^+$-binding pocket of exoenzyme C3^{Stau} is determined by Binding-Site Search module, of which the NAD$^+$-binding pockets to the enzyme has been revealed by previous experiment, and our result is in consistent with experimental fact. The NAD$^+$–enzyme complex is studied by molecular dynamics simulation and the key

residues involved in the combination of enzyme binding to the receptor of NAD^+ are defined, which is helpful for the realization of the experiment results, and guiding the new mutant designs as well. In our studies, the residues of Arg48, Asn44, Ser138, Asn134, Gln179, and Glu180 are identified for the model and these residues are important for strong hydrogen bonding interaction with substrate and play an major role in the catalysis of exoenzyme $C3^{Stau}$, which are in good agreement with the experiment by Wilde et al. The Arg85 also appear as important binding-site residue has the π–π interactions with NAD^+ for the model. These residues mentioned above may be the prime targets for site-directed mutagenesis experiments.

Acknowledgements

This work is supported by the National Science Foundation of China (29892168, 20073014), Doctor Foundation by the Ministry of Education, Foundation for University Key Teacher by the Ministry of Education, Key subject of Science and Technology by the Ministry of Education of China, and Key subject of Science and Technology by Jilin Province.

References and notes

1. Ueda, K.; Hayaishi, O. *Ann. Rev. Biochem.* **1985**, *54*, 73–100.
2. Williamson, K. C.; Moss, J. In *ADP-ribosylating Toxins and G Proteins: Insights Into Transduction*; Moss, J., Vaughan, M., Eds.; American Society for Microbiology: Washington, DC, 1990; pp 493–510.
3. Wilde, C.; Chhatwall, G. C.; Schmalzing, G.; Aktories, K.; Just, I. *J. Biol. Chem.* **2001**, *276*, 9537–9542.
4. Just, I.; Mohr, C.; Schallehn, G.; Menard, L.; Didsbury, J. R.; Vandekerckhove, J.; van Damme, J.; Aktories, K. *J. Biol. Chem.* **1992**, *267*, 10274–10280.
5. Just, I.; Selzer, J.; Jung, M.; van Damme, J.; Vandekerckhove, J.; Aktories, K. *Biochemistry* **1995**, *34*, 334–340.
6. Chardin, P.; Boquet, P.; Madaule, P.; Popoff, M. R.; Rubin, E. J.; Gill, D. M. *EMBO J.* **1989**, *8*, 1087–1092.
7. Bell, C. E.; Eisenberg, D. *Biochemistry* **1996**, *35*, 1137–1149.
8. Li, M.; Dyda, F.; Benhar, I.; Pastan, I.; Davies, D. R. *Proc. Natl. Acad. Sci. U.S.A.* **1994**, *92*, 9308–9312.
9. Chavan, A. J.; Nemoto, Y.; Narumiya, S.; Kozaki, S.; Haley, B. E. *J. Biol. Chem.* **1992**, *267*, 14866–14870.
10. Jung, M.; Just, I.; van Damme, J.; Vandekerckhove, J.; Aktories, K. *J. Biol. Chem.* **1993**, *268*, 23215–23218.
11. Takada, T.; Iida, K.; Moss, J. *J. Biol. Chem.* **1995**, *270*, 541–544.
12. Kahn, K.; Bruice, T. C. *J. Am. Chem. Soc.* **2001**, *123*, 11960–11969.
13. Wilde, C.; Just, I.; Aktories, K. *Biochemistry* **2002**, *41*, 1539–1544.
14. Han, S.; Arvai, A. S.; Clancy, S. B.; Tainer, J. A. *J. Mol. Biol.* **2001**, *305*, 95.
15. Eisenhaber, F.; Persson, B.; Argos, P. *Crit. Rev. Biochem. Mol. Biol.* **1995**, *30*, 1.
16. InsightII, Version 98.0. San Diego: MSI; 1998.
17. Dauber-Osguthorpe, P.; Roberts, V. A.; Osguthorpe, D. J.; Wolff, J.; Genest, M.; Hagler, A. T. *Proteins* **1988**, *4*, 31–47.
18. Kabsch, W.; Sander, C. *Biopolymers* **1983**, *22*, 2577–2637.
19. Homology User Guide, San Diego: MSI, USA, 1999.
20. Needleman, S. B.; Wunsch, C. D. *J. Mol. Biol.* **1970**, *48*, 443–453.
21. Discover 3 User Guide, San Diego: MSI, USA, 1999.
22. Profile-3D User Guide, San Diego: MSI, USA, 1999.
23. Luthy, R.; Bowie, J. U.; Eisenberg, D. *Nature* **1992**, *356*, 83–85.
24. Binding-Site User Guide, San Diego: MSI, USA, 1999.
25. Affinity User Guide, San Diego: MSI, USA, 1999.
26. Han, S.; Craig, J. A.; Putnam, C. D.; Carozzi, N. B.; Tainer, J. A. *Nat. Struct. Biol.* **1999**, *6*, 931.
27. Venclovas, C.; Zemla, A.; Fidelis, K.; Moult, J. *Proteins (Suppl.)* **1997**, 7–13.
28. Domenighini, M.; Rappuoli, R. *Mol. Microbiol.* **1996**, *21*, 667–674.
29. Ritter, H.; Koch-Nolte, F.; Marquez, V. E.; Schulz, G. E. *Biochemistry* **2003**, *42*, 10155–10162.
30. Carroll, S. F.; Collier, R. J. *Proc. Natl. Acad. Sci. U.S.A.* **1984**, *81*, 3307–3311.
31. Carroll, S. F.; Collier, R. J. *J. Biol. Chem.* **1987**, *262*, 8707–8711.
32. Antoine, R.; Tallett, A.; van Heyningen; Locht, C. *J. Biol. Chem.* **1993**, *268*, 24149–24155.
33. Barbieri, J. T.; Mende-Mueller, M.; Rappuoli, R.; Collier, R. J. *Infect. Immun.* **1989**, *57*, 3549–3554.
34. Payne, V. A.; Chang, Y. T.; Loew, G. H. *Proteins* **1999**, *37*, 176–190.
35. Chang, Y. T.; Loew, G. H. *Proteins* **1999**, *34*, 403–415.